# Low Vibration Design on A Helical Gear Pair

**Professor Dr. Eng. Kiyohiko Umezawa**

Helical gear pairs with narrow face width can be theoretically classified into three categories over the contact ratio domain whose abscissa is the transverse contact ratio and whose ordinate is the overlap contact ratio. There is a direct relation between vibration magnitude and shaft parallelism deviation. To clarify the effect of the tooth deviation types on the vibration behavior of helical gear pairs, performance diagrams on vibration are introduced. The acceleration levels of gear pairs are shown by contour lines on the contact ratio domain. Finally, the performance of gears with bias-in and bias-out modifications is discussed considering the effect of the shaft parallelism deviation with use of the developed simulator on a helical gear unit. It becomes clear that there is an asymmetrical feature on the relation between the vibration magnitude of a gear pair and the direction of each deviation.

***The Helix Angle and the Transmission Behaviors of a Driven Gear.*** The author numerically solved the deflections of a thick plate with finite width (Ref. 15) and a rack shaped cantilever (Ref. 16) under a concentrated load (as shown by Olsson in Ref. 1) by using the finite difference method. Furthermore, the load distribution along the line of contact and the compliance of a helical gear tooth pair from the start of meshing to the end of meshing have been revealed (Ref. 17–19).

When the face width is constant, i.e. three times the whole depth, the relation between the helix angle and the calculated behaviors of the driven gear under loading is shown in Figure 1. These results are analyzed assuming that the normal pitch $P_{tn}$, normalized with the whole depth, is 0.6. Then the whole contact ratio is calculated for each helix angle. The overlap ratio is calculated from this whole contact ratio and the assumption that the transverse contact ratio is $\varepsilon_a$=1.4. This contact ratio was calculated for a spur gear pair when the normal pitch $P_{tn}$ is 0.6

When the helix angle is 14° (Figure1a), the sum of the transverse and overlap contact ratio is smaller than 2. Therefore, this pair of gears transmits load alternately with one pair and with two pairs of mating teeth. The load sharing ratio for this pair of gears varies more smoothly than that of spur gears. But sometimes knobs appear on this curve when the meshing condition transits from one pair meshing to two pairs meshing.

When the helix angle is 20° or 30° (as shown in Figures 1c and 1d), the total contact ratio is over 2. The gears alternately transmit load with two and three mating pairs of gear teeth, the load sharing ratio varying smoothly. The behavior of the driven gear, or the transmission error, also varies smoothly. Especially when the helix angle is 30°, the overlap contact ratio is over 1.0 and the behavior changes very smoothly with little fluctuation as shown.

***Three Categories of a parallel axes gear pair.*** Theoretical and experimental studies on static meshing behavior under load have proven that a power transmission parallel gear pair can be classified into three categories on the contact ratio domain based on its facility for reducing vibration as shown Figure 2.

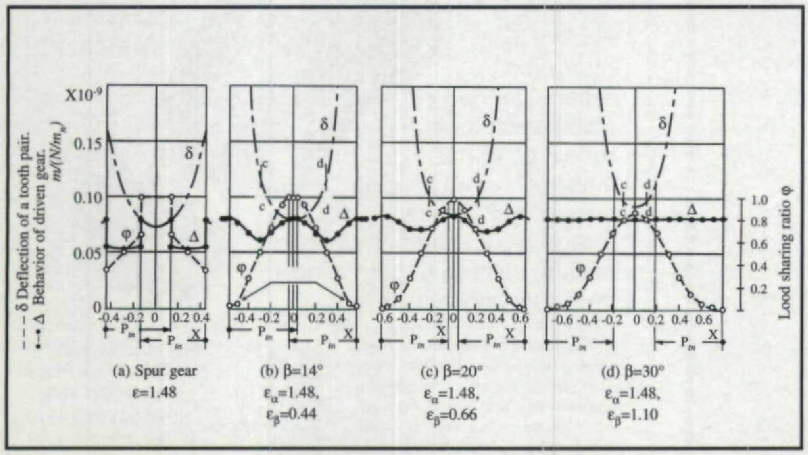


*Fig. 1—The behaviors of the driven gear and the helix angle with b/h = 3.0.*

## Vibration Magnitude and Shaft Parallelism

The relation between vibration and parallelism of axes was investigated for three kinds of helical gear pairs classified into three categories. Two kinds of shaft misalignment were implemented, in-plane and out-of-plane deviation. For realizing the out-of-plane or the in-plane parallelism, the pedestal of the driving gear shaft was tipped in the vertical plane or in the horizontal plane,

respectively. The vibration was measured by two accelerometers attached directly to the driven gear blank surface.

***Dimensions of test gears and test apparatus.*** Test gear pairs were designed to belong to each category classified over the contact ratio domain, and are named H1, H2, H3 and H4 as shown in Figure 2. Dimensions of each gear pair are displayed in Table 1. All test gears were hardened about Hrc55, and finished by the MAAG 30-BC Gear Grinder. Tooth profile and tooth traces are made with as little deviations as possible.

***Shaft misalignment set up.*** Shaft misalignment was created by placing several thickness gages on the surface of the base plate or on its side surface for the out-of-plane or in-plane deviation (Fig. 3). Thickness gages of 0.1–0.4 mm were used and the angular deviations realized were about $0.5 \times 10^{-3}$ rad and $1.1 \times 10^{-3}$ rad. The amount of the out-of-plane and the in-plane deviation was measured with two dial indicators. Gear shaft misalignment was introduced for both the leading and trailing side bearings.

***Influence of the out-of-plane deviation.*** The relation between rotational vibration response vs. speed and out-of-plane deviation for the gear pair H3 is shown in Figure 4. With proper alignment (as indicated by "no error"), acceleration increases with the speed. Being observed in the cases of the gear pairs H1 and H2, the peak cannot be recognized for these gear pairs without deviation.

When 13μm edge to edge deviation exists at the leading side, the peak appears at about 2700 rpm, which is ascribed to the second harmonic resonance. As the error increases to 29μm, acceleration increases over the whole speed range and the peak occurrence shifts towards a lower speed. However, when an error of 14μm exists on the trailing side, there is no remarkable increase in vibration. When the error increases to 30μm, peaks appear at the higher harmonic resonance, and the acceleration levels becomes high.

***Influence of the in-plane deviation.*** For the gear pair H3, the relation between the rotational vibration response and the in-plane deviation is shown in Figure 5. In the case of an error on the trailing side, the vibration of this gear pair is not influenced by the error. With an error on the leading side, the acceleration level becomes high, and higher harmonic resonance peaks appear. However, the vibration behavior of the pair is not as influenced as with the out-of-plane deviation.

**Performance Diagrams on Vibration**

To clarify the influence of tooth deviations on vibration, a simulator for the rotational vibration of a helical gear pair was developed. Performance diagrams on vibration with acceleration levels shown by contour lines on the contact ratio domain are included.

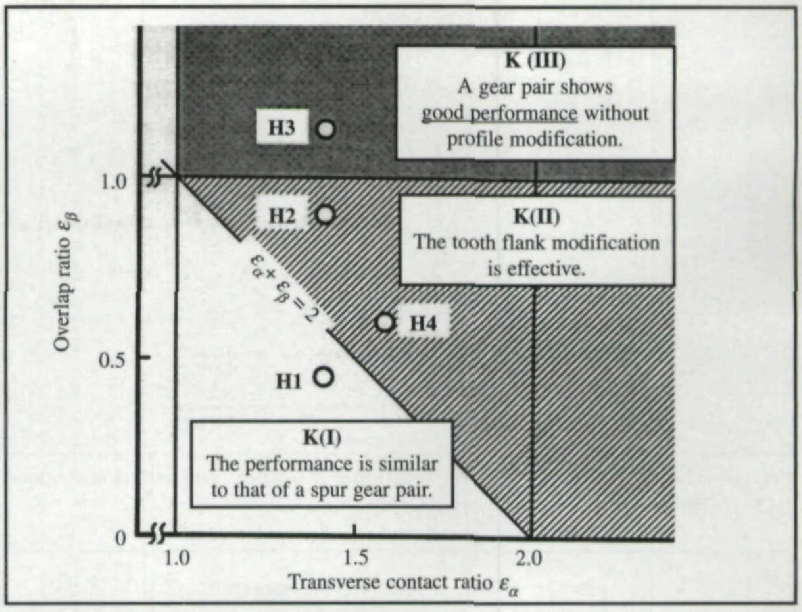


*Fig. 2—Classification of parallel pairs.*

**Table 1—Dimensions of test gear pairs.**

| Gear pair | H1 | H2 | H3 | H4 |
|---|---|---|---|---|
| Normal module | 3.5 | | | 4 |
| Number of teeth | 30 | | | 29 |
| Helix angle (deg) | 30 | | | 15 |
| Pressure angle (deg) | 20 | | | |
| Face width (mm) | 10 | 20 | 25 | 28 |
| Addendum modification coefficient | –0.17 | | | 0 |
| Transverse contact ratio | 1.4 | | | 1.57 |
| Overlap contact ratio | 0.45 | 0.91 | 1.14 | 0.58 |

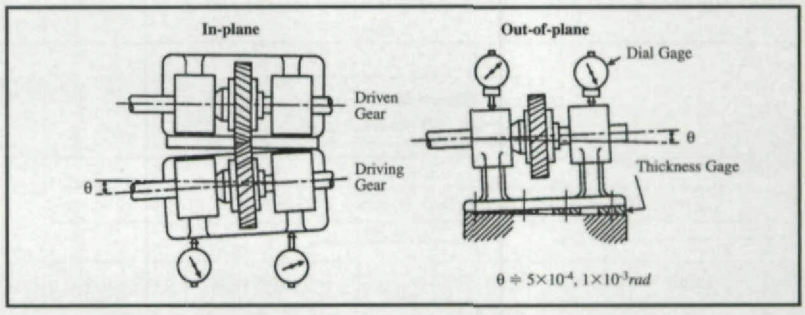


*Fig. 3—Shaft misalignment setup.*

**Theoretical Analysis on the Vibration of a Helical Gear**

***Model of motion.*** Considered along the line of action of a helical pair, imaging at the center line of the plane of action, the rotational motion of a power transmitting helical gear pair can be treated as a single degree of freedom system similar to the case of a spur gear pair, i.e., the tooth is treated as a spring and the gear blank as a mass, by the following equation.

$$M\ddot{\delta}+D\dot{\delta}+K(t,\delta)=W+F(t,\delta) \qquad (1)$$

## Dr. Kiyohiko Umezawa

*(1938-1998) was a professor in the precision and intelligence laboratory at the Tokyo Institute of Technology, Tokyo, Japan. At the Institute, he used his expertise in gear design, machine dynamics, vibration and acoustical measurement to work on reducing sound and vibration in gear units. Dr. Umezawa died suddenly at the age of 60 while on a short vacation after presenting this paper at the AGMA 1998 Fall Technical Meeting.*

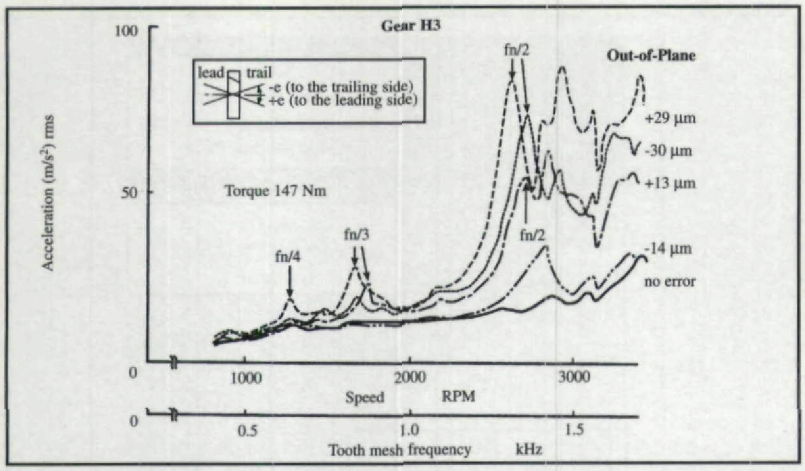


**Fig. 4—The relation between the rotational vibration and rotational speed (H3) (Influence of the out-of-plane).**

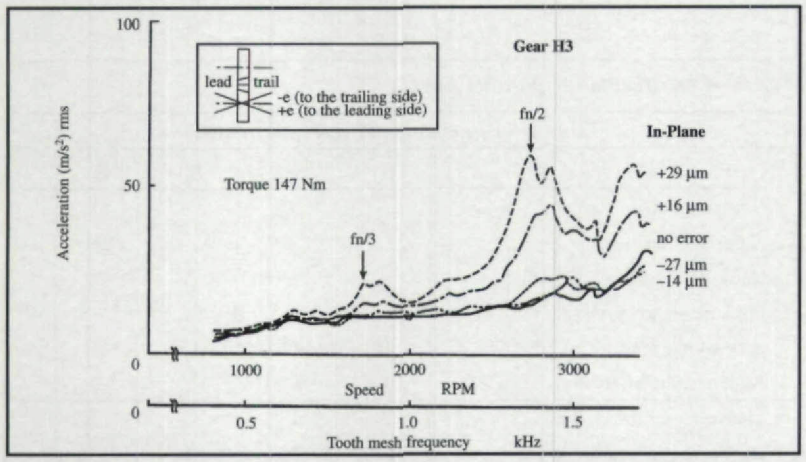


**Fig. 5—The relation between the rotational vibration and rotational speed (H3) (Influence of the in-plane deviation).**

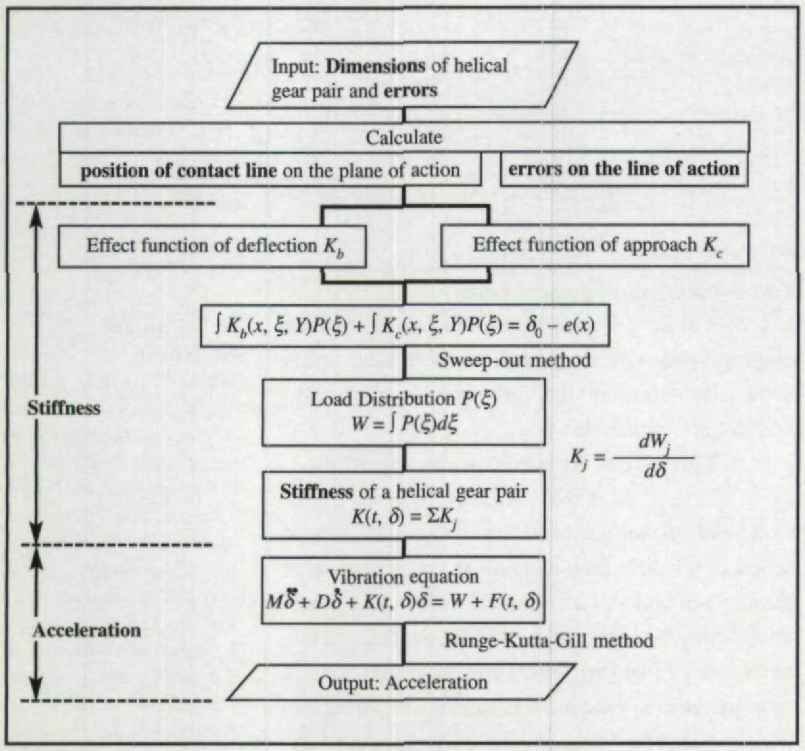


**Fig. 6—Flow chart of the developed simulator on rotational vibration of a helical pair.**

Where $\delta$ is the relative displacement along the line of action, $M$ is the equivalent inertial mass of the gear pair on the line of action, $D$ is the damping coefficient, $K(t,\delta)$ is the mesh stiffness of the gear pair; $W$ is the static transmitting load, and $F(t,\delta)$ is the exciting force caused by profile modification or deviations $\bar{e}(Y)$.

***Dimensionless acceleration.*** The motion equation of a pair expressed in Eq. (1) can be transformed into the non dimensional form,

$$\ddot{\chi}+2\zeta\sqrt{\kappa(\tau,\chi)}\dot{\chi}+\kappa(\tau,\chi)\chi=1+\phi(\tau,\chi)' \quad (2)$$

Where $\kappa(\tau,\chi)=K_i(t,\delta)/K_{i,\,mean}$ is the dimensionless stiffness of a helical gear pair, $\chi=\delta/\delta_s$ is the dimensionless relative displacement, $\delta_s = W/K$ is the mean of the relative displacement, $\phi(\tau,\chi)=F(t,\delta)/W$ is the dimensionless exciting function, $\omega_n = \sqrt{K(t)/M}$ is the natural frequency of a pair, and $\tau=t\cdot\omega_n$ is dimensionless time. When the gear speed is represented by the parameter $f_z/f_n$ (hereafter referred to as only "speed"), the nondimensional vibrational equation (Eq. 2) is solved by the use of equations shown in Figure 6.

Furthermore the dimensionless acceleration $\ddot{\chi}$ is expressed as follows,

$$\ddot{\chi} = \delta/(W/M). \quad (3)$$

The value of the dimensionless acceleration indicates the performance of the pair related to vibration in RMS value of acceleration. This value is hereafter called "the vibration level," which is obtained uniquely at each point on the contact ratio domain.

### The Developed Simulator

For solving the rotational vibration of a helical gear pair with narrow face width, a simulator was developed whose flow chart is expressed in Figure 6. It was developed especially for calculating the influence of tooth surface deviation. The input values required are only the dimensions of a helical gear pair, the distribution of deviations over the tooth face and the driving speed.

The simulator solves the differential equation with the Runge-Kutta-Gill method and outputs the vibration of the pair as either a wave form as shown in Figure 7, or a root-mean-square value of acceleration as shown in Figure 8.

***Verification by Experiments.*** Calculated and experimental results under the 98 Nm of torque, at rotational speeds from 800 rpm to 2000 rpm, are shown in Figure 7. The gear pair has a normal module of 3.5, 30 teeth each, 20° pressure angle, 10 mm face width, and a 30° helix angle with a 10µm convex slope deviation at tip-side.

Agreement between the calculated results from the simulator and experimental results is good about the waveform, especially the change in the numbers of vibration cycles within one tooth meshing period $T_z$ and about the behavior of amplitude as the rotational speed is increased.

The relation between vibration amplitude in RMS value and rotation speed is shown in Figure 8. This was developed using a good quality pair with deviations under 3μm, and whose dimensions are the same as those in Figure 7 except for the 25mm face width.

***Nature of dimensionless stiffness.*** Figure 9 shows the stiffness behaviors along the line of action $K_i(t,\delta)$ of two helical pairs, (a) and (b). These are plotted at the same position on the contact ratio domain (black dot in the lower left figure).

Apparently stiffness behavior is different, especially with respect to the mean value of stiffness $K_{i,mean}$. However, the behavior of the dimensionless stiffness $\kappa(\tau,\chi)$, in which the actual stiffness is divided by the mean value of stiffness, is the same as shown Figure 9(c) from the viewpoint of how to synthesize the performance of helical gear pairs because the differences among the first order Fourier coefficients of each dimensionless stiffness are within 10 percent deviation on each pair belonging at the identical point on the contact ratio domain. The differences of the higher order Fourier coefficients are of the same level amplitude, and their values are smaller by one third than coefficients of the first.

***Performance diagrams on vibration of helical gears.*** At each operating speed and under each deviation condition, the vibration levels were solved numerically by the simulator at 80 points in the contact ratio domain, where the transverse contact ratio (abscissa) was set at 8 points from 1.0 to 2.0 and the overlap ratio (ordinate) was at 10 points from 0.2 to 2.3. Consequently, the solved vibration levels were expressed as contour lines on the contact ratio domain.

***Accounted deviations and modifications.*** Performance diagrams were produced on the seven kinds of pairs: the no error pair, the pair with crowned tooth face, and the pairs having, respectively, pressure angle (profile slope deviation in ISO), convex profile, concave profile, lead and pitch deviations, which are similar in manufacturing and assembling gear units. The performance diagrams calculated under the condition that the relative deviations between meshing driving and driven teeth are gathered apparently to only driven gear teeth, which have ideally the same figure and the same amount of deviations for every tooth in the gear. Therefore all teeth of the driving gear have ideally no error for calculation.

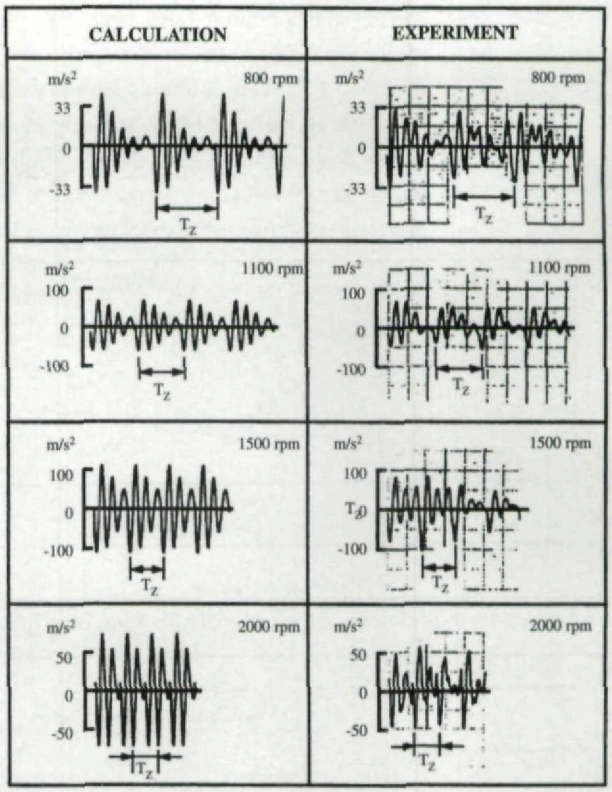


**Fig. 7—Verification by experiments on the changing speed.**

***Performance diagrams on a non-error pair.*** The produced performance diagrams on a pair having no error at each speed $f_z/f_n$ changing from a low value of 0.21 to a high value 0.98. The interval of vibration level between adjacent contour lines is a 0.025 vibration level. Generally, at each speed the vibration level becomes small according to an increase in overlap contact ratio, except for the 2nd resonance speed ($f_z/f_n$ = 0.49) and the high speed region.

***At low speed*** ($f_z/f_n \leq 0.35$). There is no difference in the vibration level of pairs belonging in this area by the scale 0.025. Clearly, choosing an overlap ratio over 1.0 lowers the vibration of a helical gear pair.

***At middle speed*** ($0.35 < f_z/f_n \leq 0.7$). In the area $\varepsilon_\beta < 1.0$, the vibration level decreases when the transverse contact ratio $\varepsilon_\alpha = 2.0$. The contour lines trace along the band which is 45 degrees to each coordinate and where the total contact ratio $\varepsilon_\gamma$ is 2.1. When designing a low vibration helical gear pair, the pair should be categorized into the upper side of this bank. On the middle speed, the vibration of a helical gear pair can be reduced by setting its total ratio over 2.1. The diagram of $f_z/f_n = 0.49$ showed complicated and dense contour lines because $f_z/f_n = 0.49$ is near the 2nd harmonic resonance speed.

***At high speed*** ($0.7<f_z/f_n\leq 1.0$). In the area $\varepsilon_\beta<1.0$, the vibration level becomes large, especially around a transverse contact ratio of $\varepsilon_a=1.5\sim1.6$. It then decreases around $\varepsilon_a=2.0$.

In the area of $\varepsilon_\beta>1.0$, where vibration is weak at low and middle speeds, the vibration strengthens in the area of $\varepsilon_\beta=1.3$ and $\varepsilon_a=1.5$. Moreover, a strong vibration area extends around the total contact ratio $\varepsilon_\gamma=2.9\sim3.0$. This indicates that the vibration of a pair having no error is determined only by the behavior of the stiffness of a pair in Eq. 2. Therefore, the performance diagram at $f_z/f_n=0.91$ is very similar to the equi-amplitude contours of first order component of the Fourier series of stiffness. It is reasonable that the contour lines become dense and high at $f_z/f_n=0.98$ because it is near to the resonance speed.

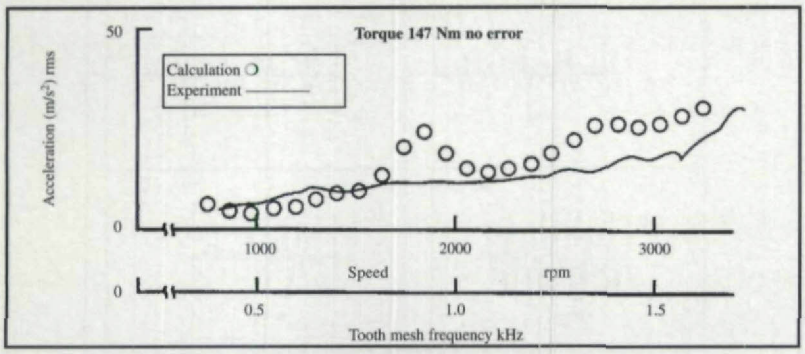


**Fig. 8—Verification by experiments on rotational vibration (rms) vs. speed.**

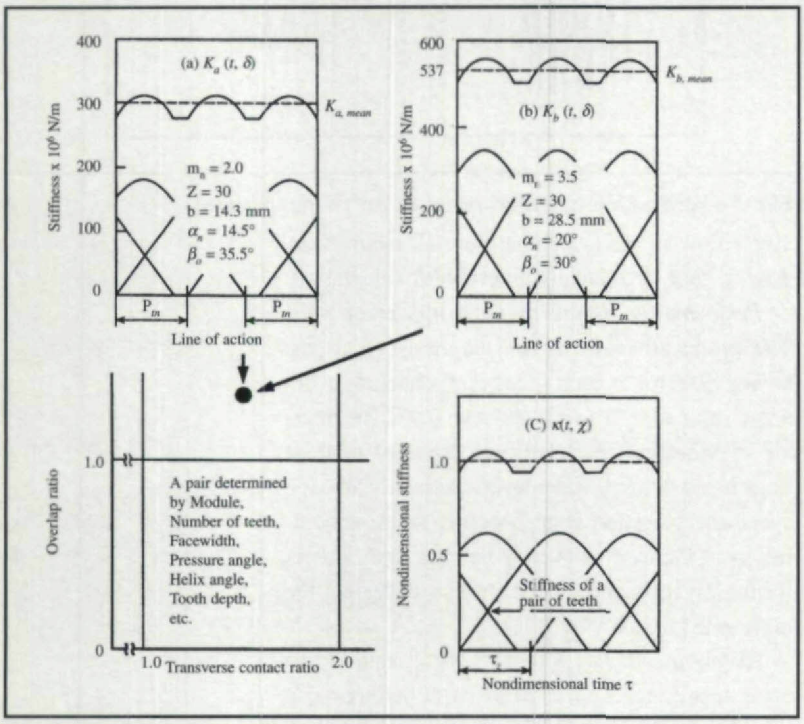


**Fig. 9—The nature of stiffness of the pairs having the same contact ratio.**

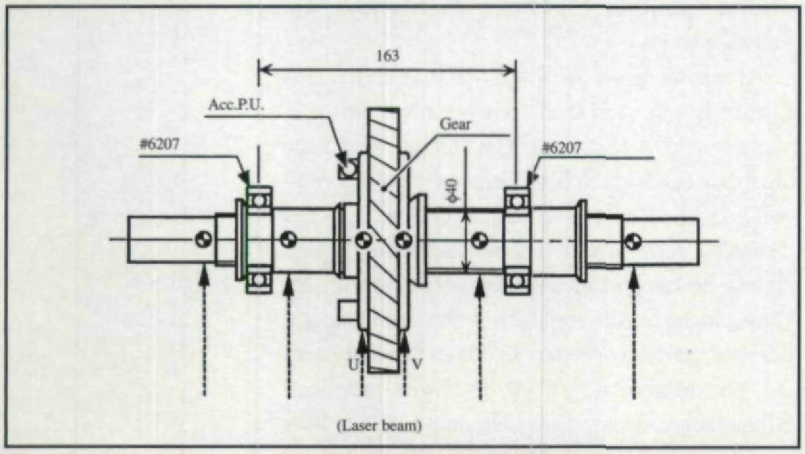


**Fig. 10—Measurement points of laser Doppler velocimeter.**

***Performance diagrams on a pair having each kind of deviation.*** The performance diagrams on vibration were drawn at the speeds $f_z/f_n=0.63$ and $f_z/f_n=0.98$. Each diagram was calculated with every tooth on the driven gear having the same deviation, and the nondimensional deviation was 1.0. The maximum deviation is set to be the same as the mean deformation produced by the transmitting load.

***At middle speed*** ($f_z/f_n=0.63$). In the diagram on pitch error (single pitch deviation in ISO), the contour lines become parallel to the direction, 45 degrees to each coordinate, at which the total contact ratio is constant. The vibration does not increase much in the area of $\varepsilon_\beta>1.0$, almost regardless of the deviation. This feature is understood because the pitch deviation is assumed to be the same on every other tooth, so the load is always transmitted by the projecting area of every other tooth, therefore, apparently having little effect of pitch deviation. Increasing the total contact ratio of a pair weakens the influence of pitch deviation on increasing vibration.

***At high speed*** ($f_z/f_n=0.98$). In the high speed diagram, the contour lines generally become denser than those at the middle speed. Therefore, the vibration of a pair increases over all the area in the contact ratio domain.

On the pair having a convex profile, the vibration increases in the area of $\varepsilon_\alpha<1.4$. On the area of $\varepsilon_\alpha=1.4\sim1.6$ and $\varepsilon_\beta>1.2$, the vibration level decreases because the convex profile works as a profile modification.

On the pair having a concave profile, over the entire contact ratio domain, the vibration level increases in comparison with the pair with no error. It is also especially large in the area ($\varepsilon_\alpha$, $\varepsilon_\beta$)=(1.5, 1.5), where the vibration of the pair having the other deviations is small.

On the pair having a lead error (helix deviation in ISO), the vibration level increases around $\varepsilon_\alpha=1.5$ and also in several regions over $\varepsilon_\beta>1.0$ where the vibration is usually low. The nature is different from one of a pressure angle error, although the lead deviation and pressure angle deviation look the same as the projecting deviation at the beginning of the mesh process. However, they work differently

along the line of contact of a helical gear and cause vibration.

When the tooth surface is crowned, vibration in the range of $\varepsilon_\beta \geq 1.0$ decreases in comparison with the pair with no error.

The simulator can depict vibration levels and waveform behavior precisely. The performance diagrams depicted the influence of deviation and operating speed on the vibration level of a pair in the contact ratio domain. Using these diagrams, a designer can select the best dimensions to lower the vibration of a newly designed gear to the lowest vibration or influence area by the use of deviations. Also, when an engineer has to improve a noisy gear, he can choose the most effective improvement by crossing to the contour lines of the diagrams.

**Bias Modification**

Finally, bias-in and bias-out modifications are discussed as they relate to shaft parallelism deviation with the use of the simulator on a helical gear unit (Ref. 23).

Among gear vibrations, rotational vibration is the most important. It can be approximated with a single-degree-of-freedom model. However, the effect of the thrust force from the helix angle of a helical gear complicates the vibration of a gear unit. To further reduce vibration, it is important to reveal the actual modal behaviors of the gear vibrations in every direction as well as the vibrations of the shafts.

The vibration of a helical gear unit as shown in Figure 10 with various gear ratios has been investigated. The dynamic response of transverse, rotational, tilting and axial vibrations of helical gears are measured by acceleration pick-ups mounted on the gear blank. Modal behavior is interpreted based on a modulation scheme due to shaft rotation. The modes of shafts and gears are measured precisely with a laser Doppler velocimeter. Then the simulation on a dynamic model, including transverse, rotational, tilting, and axial vibrations, is developed.

***Modal Behavior.*** The locus of the transverse motion of the gears and gear shafts, measured with a laser Doppler velocimeter at resonance, are presented as q and Q in Figure 11. Circle marks are the points of instantaneous displacement when the rotation of the gear is such that the separation of the gears is the greatest along the line of action. Triangles are the spots of the opposite condition. Arrows indicate the direction of motion. Additionally, tilting motion of the gear is presented through the differentiation of two measurements at both shoulders (U and V in Figure 13) of the gear body.

Regardless of the ratio, the shaft of the bigger gear vibrates with an S-shaped mode. Each part whirls along a thin, elliptic locus with the mesh frequency. The major axis of this ellipse is not parallel to the line of action. At the bearing position, where the motion should be interpolated from the results of both sides, a low amplitude vibration exists, suggesting that the bearing positions are not constrained as simply supported pivots. The modal behavior is also unique to an individual gear-shaft-bearing assembly regardless of driving/driven conditions. Displacement of the pinion shaft at the slip ring side bearing is a little larger than at other bearing positions. This might be an individual feature of each bearing. Although the shafts are vibrating in an interesting manner, the gear itself is supposed to move in the direction of the line of action if we assume the vibration of the gear center by interpolating with outer vibration.

***The simulator of 12-degree-of-freedom.*** To predict the vibration behaviors of helical gears as shown in Figure 14, the author proposes a 12-degree-of-freedom dynamic model that includes rotational, transverse, tilting, and axial motions. A gear is assumed to be a rigid body which can be vibrating in six directions in terms of equivalent stiffness and effective masses including the dynamic properties of gear, shafts and bearings. Tooth meshing springs of two coupled gears are modeled as two parallel springs that vary temporally with a certain phase relationship due to the helix angle.

***Vibration analysis.*** Figure 12 shows that transverse vibration can be expressed by dynamic behaviors in the $x$ and $y$ directions. Rotational vibration can be expressed in the $\theta_z$ direction.

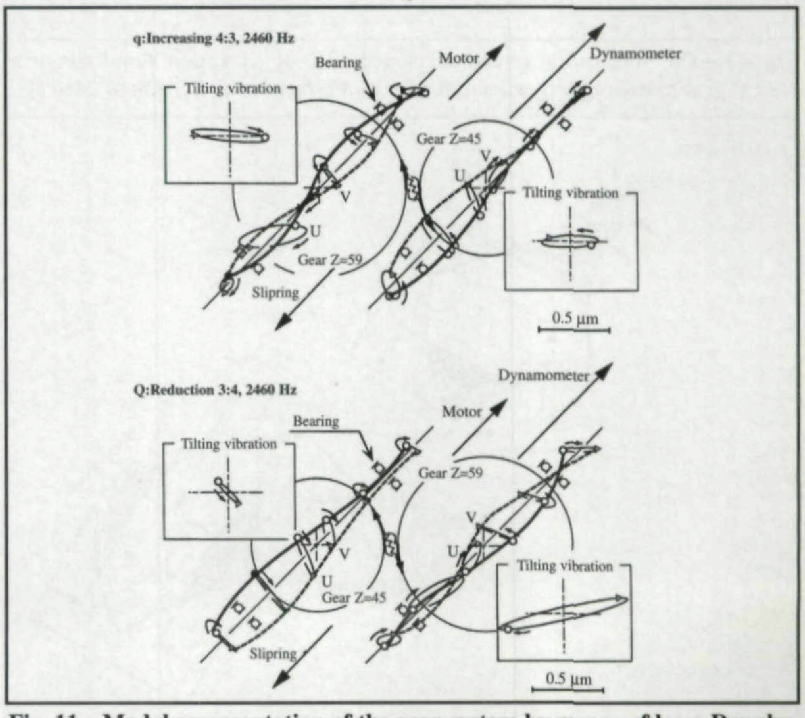


**Fig. 11—Modal representation of the gear system by means of laser Doppler measurement. Gear ratio 3:4.**

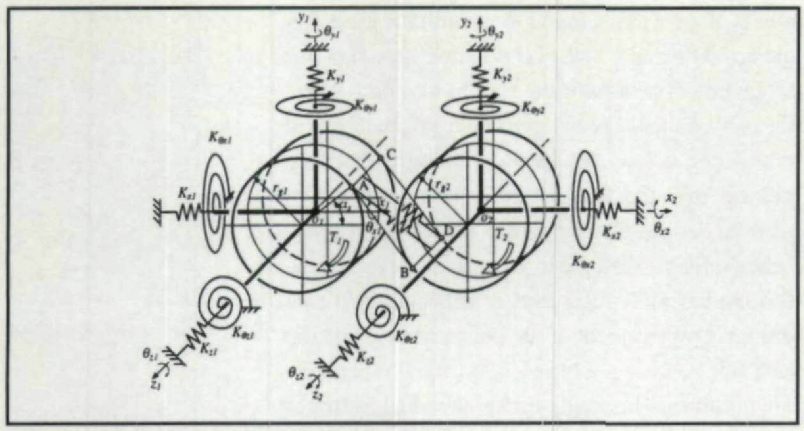

**Fig. 12—Vibration model of helical gears.**

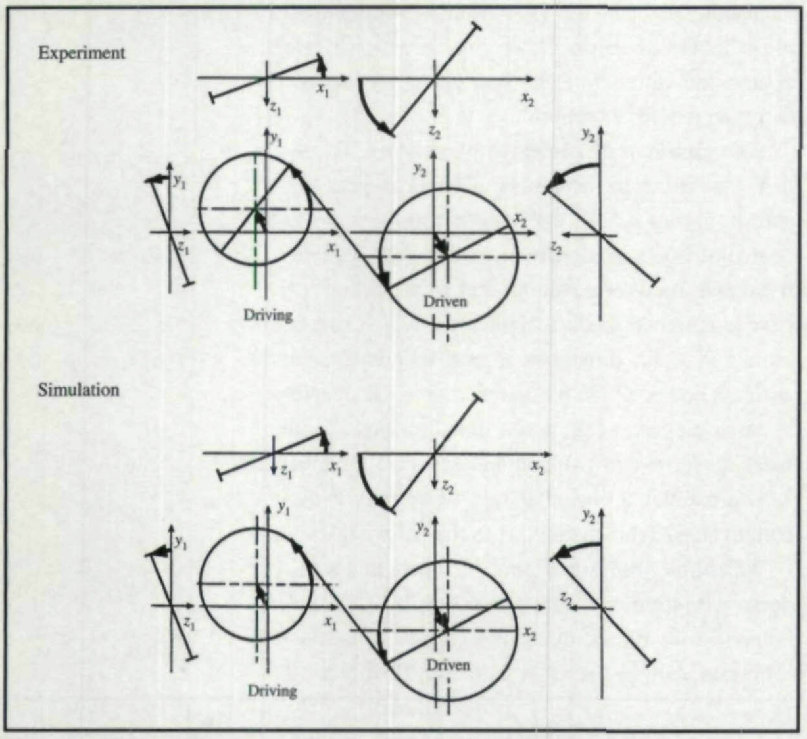


**Fig. 13—The verification of the developed 12-DOF vibration simulator of a helical gear system by experiment modes under increasing 4:3, about 2460 Hz.**

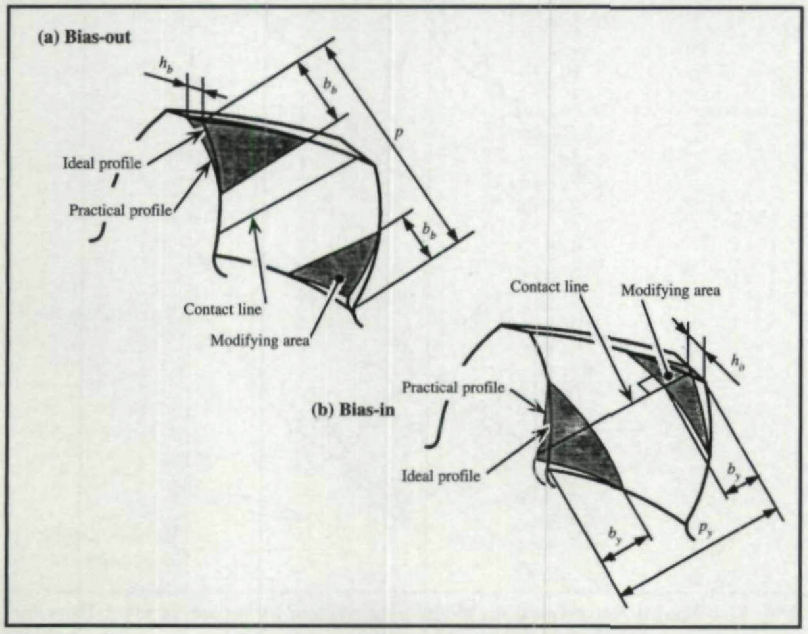


**Fig. 14—Bias-out and Bias-in modification.**

Tilting vibration can be expressed in the $\theta_x$ and $\theta_y$ directions, and axial vibration can be expressed in the $z$ direction. In each direction, the equivalent stiffness and effective mass are determined by the gear, shaft, and bearings.

Angular displacement in the rotational direction $\theta_z$ is expressed in terms of tangential displacement along the base circle as $w = r_g\theta_z$. Angular displacements in the tilting directions $\theta_x$ and $\theta_y$ are also expressed along the base circle as $u = r_g\theta_x$, $v = r_g\theta_y$. The equations of motion can be expressed in the matrix equation

$$[m]\{\ddot{\delta}\}+[D]\{\dot{\delta}\}+[k]\{\delta\}=\{F\} \quad (4)$$

Where $\{\delta\}$ is a vector of displacements as

$$\{\delta\} = \{ x_1, y_1, z_1, u_1, v_1, w_1, x_2, y_2, z_2, u_2, v_2, w_2\}^T \quad (5)$$

$[m]$ is a mass matrix, $[D]$ is a damping matrix, and $[k]$ is a stiffness matrix.

To verify the simulator with the use of the proposed formulation, experiments were performed for different ratios. The results agreed with the calculations (see Figure 13). The mode at resonance speed was found to be $f_z$ = 2460 Hz when the gear ratio is 4:3.

***The performance of a bias-modified helical gear pair.*** To decrease vibration, bias modification is often applied to the tooth surface. There are two methods in bias modification, bias-in and bias-out (see Figure 14). It is not clear which modification is better.

Using the vibration simulator of a 12-degree-of-freedom helical gear unit, the relationship between the performance of vibration level and misalignment is discussed on the bias-in and the bias-out modified helical gear pairs. These pairs have a high total contact ratio $\varepsilon = 3.81$ (usually used in automobile transmissions) to realize low vibration level. The gear data is: $z_1$ and $z_2 = 52$, $m_n = 2.0$, $\alpha$=20° and $\beta_0 = 30°$, face width 30 mm and load 133 N/mm.

Misalignment is defined as positive when the axis inclines to the leading side bearing. On the bias-out modification with misalignment from –20μ to 10μm, amplitide factor contour maps have been developed in which the abscissa is the dimensionless modification length $b_b/p$, and the ordinate is the bias modification $h_b$[μm] (see Figure 14).

The contour lines in the maps show a ratio of rotational vibration to that of a non-modified helical gear pair at the resonance speed. The influence of the amount of bias-out modification and modification length on vibration can be obtained using

the contour lines on each amplitude factor contour map. The influence of misalignment on vibration is realized by comparing the maps to each other.

## Conclusion

The proposed classification of a parallel gear pair and contact ratio domain are verified to be useful in the design of a quiet gear pair.

Our research has shown that there is an asymmetrical relationship between vibration magnitude and the direction of each deviation (see Figures 4 and 5). For further noise reduction, the effects of shaft, bearing and gear-box on vibration are of great importance.

Finally, there is no new knowledge on how to design a quiet parallel gear. However, it is clear that surface deviation, as well as the direction of that deviation, can affect the vibration level of a gear pair. Gear engineers should see that their products turn in the right direction. They are very similar men who walk step by step carefully the narrow ridge between high mountains. ⚙

**References:**


1. Olsson, R.G. "Biegung der Rechteckplatte bei linear veranderlicher Biegungssteifigkeit," Ingenieur-Archiv, Vol. 5, (1934), pp.363-373.
2. Walker, H. "Helical Gears," *The Engineer*, (1946), July 12, pp.24-26: July 19, pp.46-48: July, 26, pp.70-71.
3. Jaramillo, T.J. "Deflections and moments Due to a Concentrated Load on a Cantilever Plate of Infinite Length," *Journal of Applied Mechanics*, (1950), pp.67-72.
4. Davis, A.W. "Marine Reduction Gearing," TheTwenty-eighth Thomas Lowe Gray Lecture, *Engineering*, Vol. 201, (1956), pp.477-498.
5. Monck, E. Roy, A.K. "Spannungsoptische Untersuchung eines schragverzahnten Stimrades," Konstraction, 9, Heft 11 (1957), pp.429-438.
6. Trbojevic, M.D. "Load Distribution on Helical Gear Teeth," *The Engineer*, (1957), Aug. 9, pp187-190; Aug. 16 pp.222-224.
7. Wellauer, E.J., Seireg, A.G. "Bending Strength of Gear Teeth by Cantilever-Plate Theory," *Trans-actions of the ASME Journal of Engineering for Industry*, Paper No. 59-A-50, (1960), pp. 1-8.
8. Hayashi, K. "Load Distribution on the Contacu Line of Helical Gear Teeth (1st Report, Basic Investigation)," *Trans. Jpn.Soc. Mech. Eng.* (in Japanese), Vol. 28, No. 193, (1962), pp.1093/1101.
9. Niemann, G. und Hosel, T. "Gerauschuntersuchungen an schragverzahnten Stirnradern Einflu ( von Drehzahl und Belastung," Verzahnungsdaten und Zahnfehiern, Konstruktion, 18, Heft 4, (1966), pp. 129-141.
10. Niemann, G. und Baethge, J. "Drehwegfeler, Zahnfederharte und Gerausch bei Stimradem," VDE-Z 112, Nr.8, (1970), pp. 495-499.
11. Houser, D.R. Seireg, A. "An Experimental Investigation of Dynamic Factors in Spur and Helical Gears," *Transactions of the ASME Journal of Engineering for Industry*, (1970), pp.495-503.
12. Seireg, A., Houser, D.R. "Evaulation of Dynamic Factors for Spur and Helical Gears," *Transactions of the ASME Journal of Engineering for Industry*. (1970), pp.504-515.
13. Conry, T.F., Seireg, A. "A Mathematical Programming Method for Design of Elastic Bodies in Contact," *Transactions of the ASME Journal of Applied Mechanics* (1971), pp.387-392.
14. Conry, T.F., Seireg, A. "A Mathematical Programming Technique for the Evaluation of Load Distribution and Optimal Modifications for Gear Systems," *Transactions of the ASME Journal of Engineering for Industry*, (1973), pp.1115-1122.
15. Umezawa, K., et al. *Trans Jpn. Soc. Mech. Eng.* (in Japanese), Vol.35, No.270, (1969-2), pp.423/431.
16. Umezawa, K. "Deflections and Moments Due to a Concentrated Load on a Rack-Shaped Cantilever Plate with Finite Width for Gears," *Bull. JSME*, Vol.15, No. 79,(1972), pp.116-130.
17. Umezawa, K. "The Meshing Test on Helical Gears under Load Transmission (1st Report, The Approximate Formula for Deflections of Gear Tooth)," *Bull. JSME*, Vol. 15, No. 90, (1972), pp.1632-1639.
18. Umezawa, K. "Deflection Due to Contact between Gear Teeth with Finite Width," *Bull. JSME*, Vol. 16, No.97, (1973), pp.1085-1093.
19. Umezawa, K. "The Meshing Test on Helical Gears under load Transmission (3rd Report, The Static Behaviors of Driven Gear)," *Bull. JSME*, Vol.17, No. 112, (1974-10), pp.1348-1355.
20. Umezawa, K, Suzuki, T., Houjoh, H. and Sato, T. "Vibration of Power Transmission Helical Gears (The effect of contact ratio on the vibration)," *Bull. JSME*, Vol. 28, No. 238 (1984), pp. 694-700.
21. Umezawa, K, Suzuki, T., Houjoh, H. and Bagiasna, K. "Influence of Misalignment on Vibration of Helical Gears," *Proc. of 2nd World Congress on Gearing*, Paris, France, Vol. 1 (1985), pp. 615-626.
22. Umezawa, K. "The Performance Diagrams for the Vibration of Helical Gears," *Proc. of 1989 Int. Power Transmission and Gearing Conf.*, Chicago, Illinois, Vol. 1, (1989), pp. 399-408.
23. Wang, S., Umezawa, K., Houjoh, H. and Matsumura, S. "An Analytical Investigation of the Dynamic Behavior of a Helical Gear System," *Proc. of 7th Int. Power Transmission and Gearing Conf.*, San Diego, California, Vol. 88, (1996), pp. 169-176.
24. Umezawa, K., Houjoh, H., Matsumura, S., Wang, S. and Ohshima, S. "Experimental Investigation on Modal Behavior of Helical Gear Units with Various Ratio," *Proc. of 7th Int. Power Transmission and Gearing Conf.*, San Diego, California, Vol. 88 (1996), pp. 509-517.
25. Umezawa, K., Wang, S., Houjoh, H., and Matsumura, S. "Investigation of the Dynamic Behavior of a Helical Gear System (4th Report, Dynamics of Gear Pairs with Bias Modification)," *Trans. Jpn. Soc. Mech. Eng.* (in Japanese), Vol. 64, No. 620 (1998), pp. 1414-1420.



**A version of this article first appeared as technical paper 98FTM5 at the 1998 AGMA Fall Technical Meeting. We'd like to express our thanks to Dr. Haruo Houjoh, of the Tokyo Institute of Technology, as well as the Umezawa family, for their assistance in preparing this article.**